

Supplementary Information

Allosteric inhibition of α -thrombin enzymatic activity with ultrasmall gold nanoparticles

André L. Lira¹, Rodrigo S. Ferreira¹, Ricardo J.S. Torquato¹,

Maria Luiza V. Oliva¹, Peter Schuck², Alioscka A. Sousa^{1,*}

1. Department of Biochemistry, Federal University of São Paulo, São Paulo, SP, Brazil

2. National Institute of Biomedical Imaging and Bioengineering, National Institutes of Health, Bethesda, MD, USA

* Corresponding author: alioscka.sousa@unifesp.br

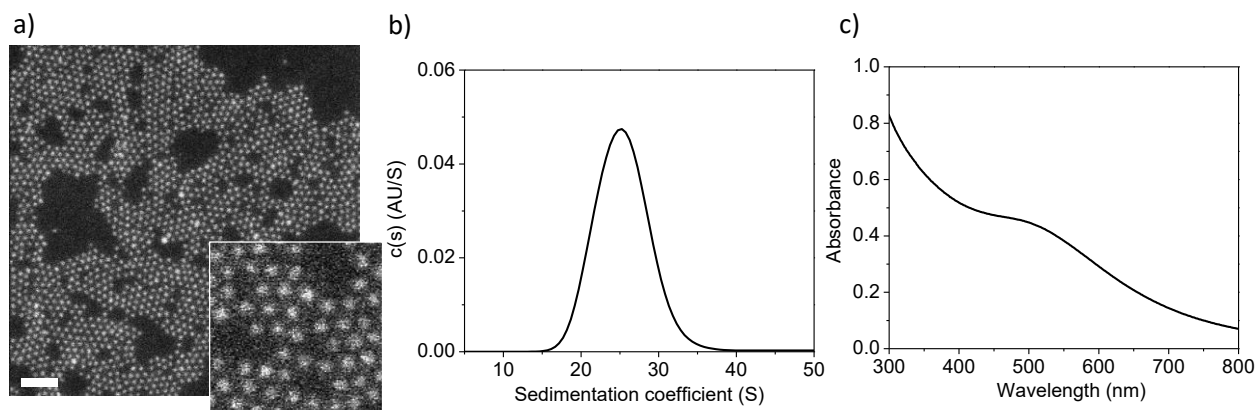


Figure S1. Characterization of AuMBA size and uniformity. (a) High-angle annular dark-field scanning transmission electron microscopy (HAADF STEM) image of ultrasmall AuMBA. The NPs appear uniform and with a gold core diameter ~ 2 nm. Scale bar, 20 nm. (b) Analytical ultracentrifugation analysis of AuMBA. The range of sedimentation coefficients displayed is consistent with particles sizes ~ 2.5 nm, in good agreement with the STEM data. (c) UV-visible spectrum of AuMBA. The spectrum shows lack of a prominent surface plasmon peak around 500 nm, consistent with the small size of the particles.

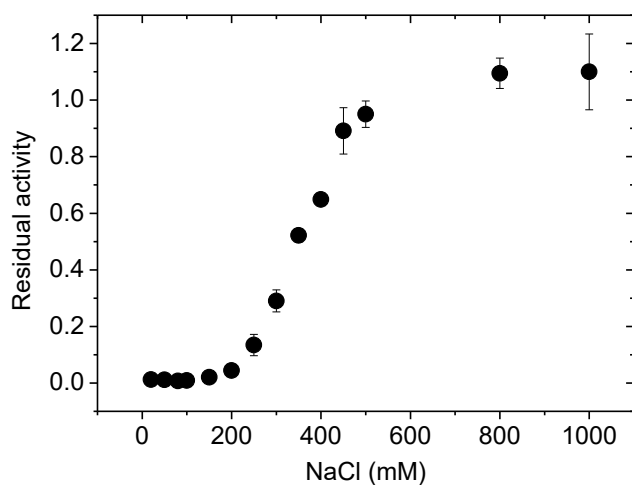


Figure S2. Dependence of AuMBA-thrombin complexation on solution ionic strength evaluated by a separation experiment. Thrombin was mixed with magnetic beads containing immobilized AuMBA under different NaCl concentrations. After separating the beads with a magnet, the presence of unbound thrombin in the supernatant was evaluated by recording the initial velocity of substrate cleavage (v_0). Values of v_0 were normalized relative to thrombin in solution without beads. Thrombin concentration, 20 nM; immobilized AuMBA, ~ 2 μ M; substrate S-2238, 100 μ M.

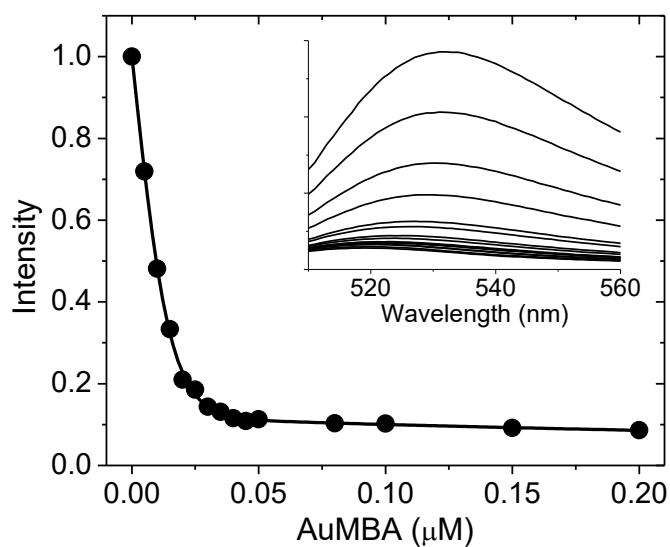


Figure S3. Fluorescence titration quenching of FITC-labeled thrombin ($0.05 \mu\text{M}$) with AuMBA in phosphate buffer solution supplemented with 150 mM NaCl . Inset: raw fluorescence spectra; the AuMBA concentration increases from top to bottom.

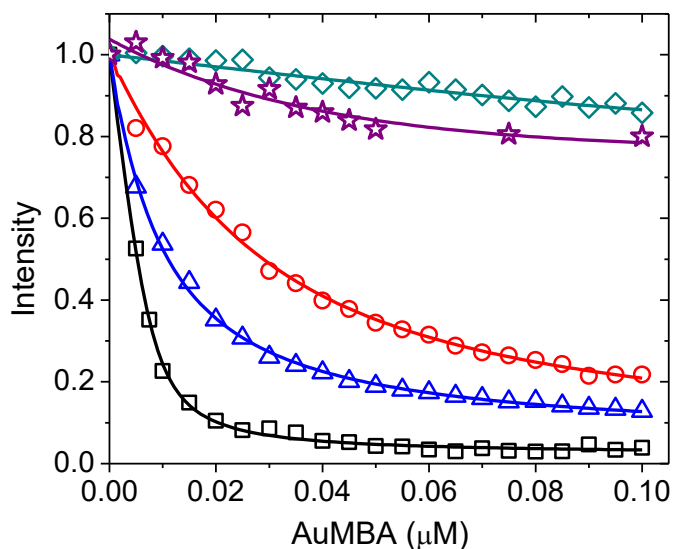


Figure S4. Fluorescence titration quenching of FITC-labeled thrombin with AuMBA in the absence (squares) and presence of excess HD1 (triangles), HD22 (circles), HD1+HD22 (diamonds), and hirudin+HD22 (stars). Thrombin concentration, $0.05 \mu\text{M}$; HD1 and hirudin, $15 \mu\text{M}$; HD22, $5 \mu\text{M}$. Assays performed in phosphate buffer solution supplemented with 150 mM NaCl . Lines are a guide to the eye.

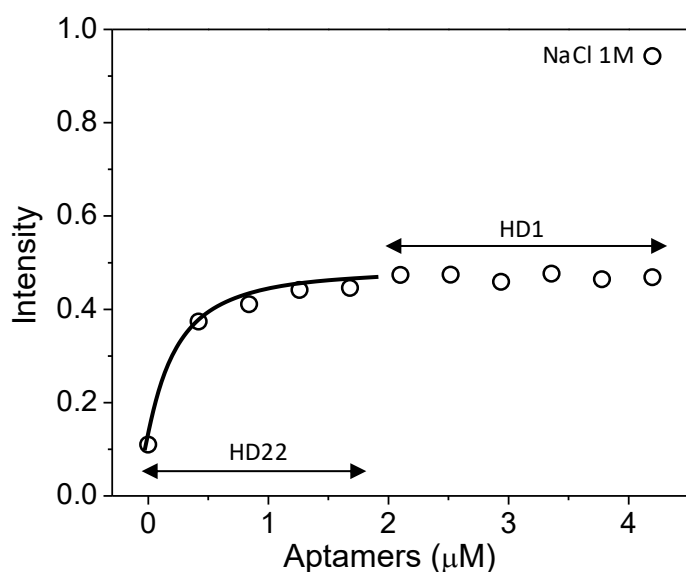


Figure S5. Recovery of γ -thrombin fluorescence by titration of γ -thrombin+AuMBA with aptamers. The NaCl concentration was increased from 150 mM to 1 M NaCl after the last titration point.

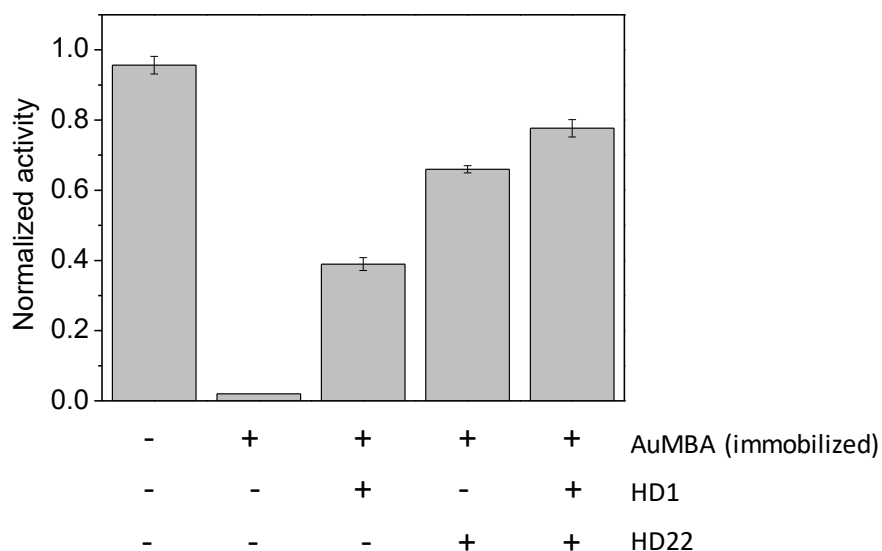


Figure S6. AuMBA-thrombin interactions in the presence of aptamers evaluated by pull-down experiments. Thrombin was mixed with magnetic beads containing immobilized AuMBA. After separating the beads with a magnet, the presence of unbound thrombin in the supernatant was evaluated by recording the initial velocity of substrate cleavage (v_0). The values of v_0 were normalized relative to thrombin in solution without beads. As a control, thrombin showed negligible binding to beads without immobilized NPs (first column). Thrombin concentration, 20 nM; immobilized AuMBA, $\sim 2 \mu\text{M}$; HD1, 20 μM ; HD22, 6 μM . Assay performed in phosphate buffer solution supplemented with 150 mM NaCl.

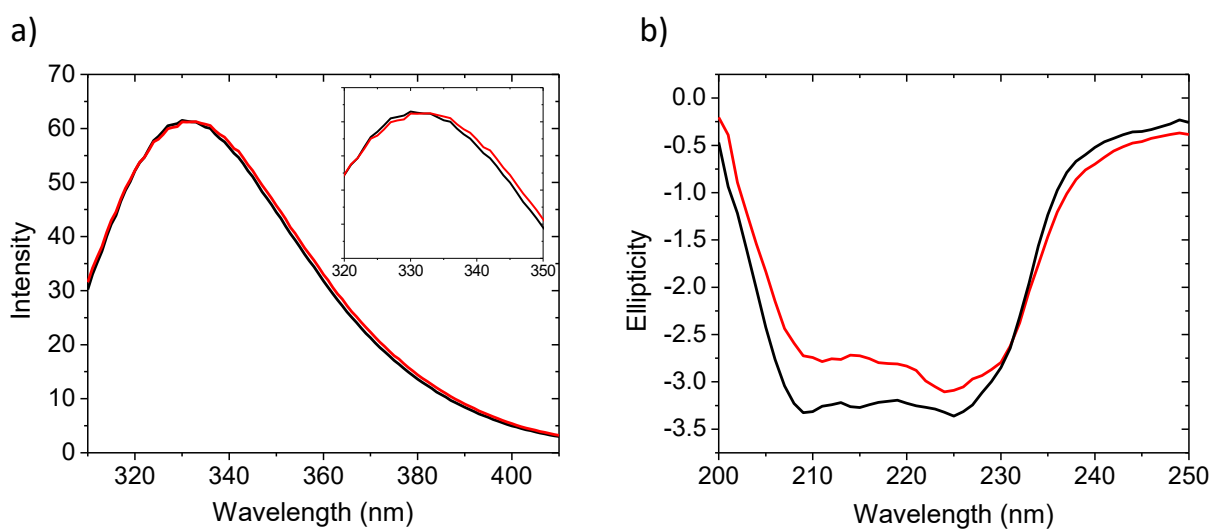


Figure S7. Global structural changes in thrombin upon interactions with AuMBA. (a) Tryptophan emission spectra of free thrombin (black) and AuMBA-bound thrombin (red). A small red-shift (~ 2 nm) in the spectrum for AuMBA-bound thrombin is apparent (inset). Thrombin concentration, $1 \mu\text{M}$; AuMBA, $0.3 \mu\text{M}$. (b) CD spectra of free thrombin (black) and AuMBA-bound thrombin. Thrombin concentration, $3 \mu\text{M}$; AuMBA, $1 \mu\text{M}$. Assays performed in phosphate buffer solution supplemented with 150 mM NaCl .

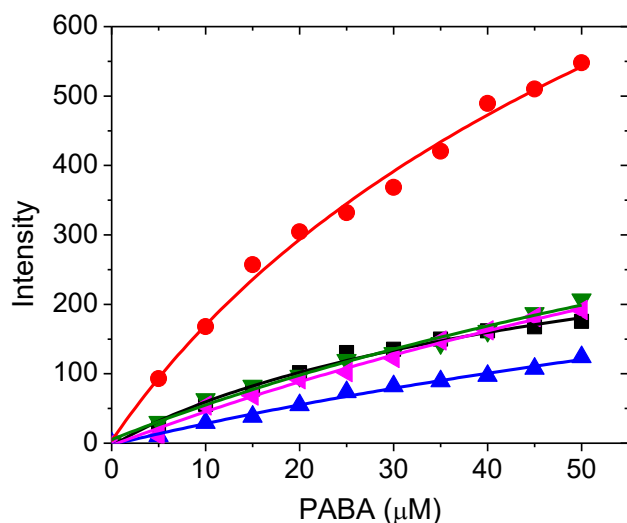


Figure S8. Binding of PABA into the active site of thrombin assessed by fluorescence spectroscopy. Measurements of PABA fluorescence were performed under the following conditions: in buffer solution without AuMBA or thrombin (black squares); in the presence of AuMBA (blue triangles); in the presence of thrombin (red circles); in the presence of thrombin inhibited with PPACK (magenta triangles); in the presence of thrombin and AuMBA (green triangles). The blue trace has lower intensity than the black trace due to the inner filter effect from the NPs. The red trace has much higher intensity than the black trace due to the larger fluorescence quantum yield of PABA when bound to thrombin. As a control, the magenta trace was observed to have the same intensity as the black trace, consistent with lack of PABA binding to PPACK-thrombin. The higher signal intensity of the green trace relative to the blue trace therefore provides evidence of PABA binding into the active site of AuMBA-bound thrombin. (It must be recalled that PABA fluorescence in AuMBA-bound thrombin will be highly quenched due to the proximity of PABA to the NPs, which explains the much lower signal of the green trace relative the red trace). Thrombin concentration, 0.5 μM ; AuMBA, 1 μM ; assay performed in phosphate buffer solution supplemented with 150 mM NaCl; the excitation and emission wavelengths were 345 and 370 nm, respectively. Lines are a guide to the eye.

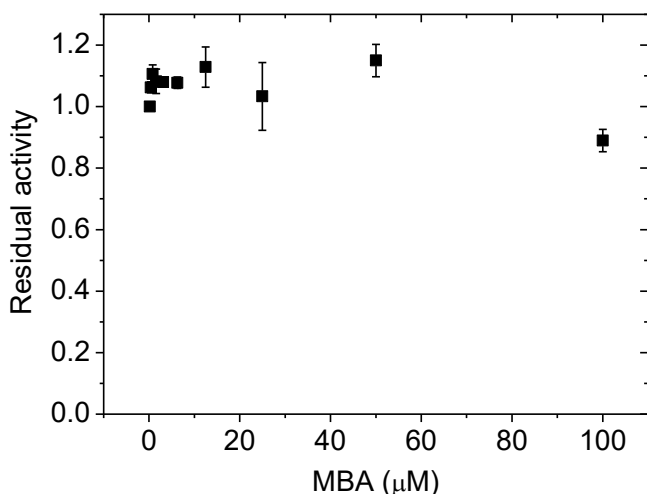


Figure S9. Concentration-dependent inhibition of thrombin by free MBA molecules. Because MBA is insoluble in water at pH 7, it was first dissolved in DMSO before being diluted further in the working buffer solution. Thrombin concentration, 2 nM; assay performed in Tris-HCl buffer solution supplemented with 100 mM NaCl; concentration of DMSO in the buffer ~ 1%.

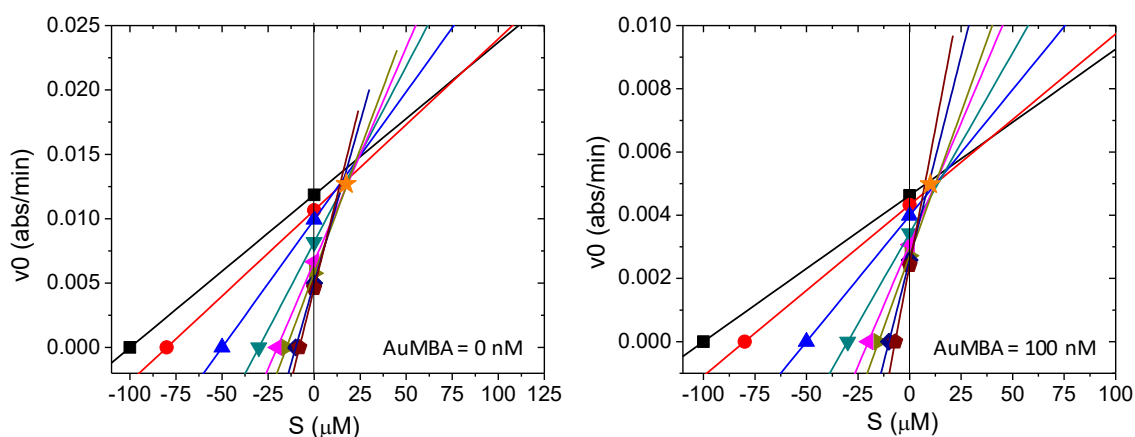


Figure S10. Determination of K_m and V_{max} by the direct linear plot method. The plot is built by placing the experimentally measured $[S]$ on the negative side of the abscissa and v_0 on the ordinate. Next, lines are drawn connecting each v_0 and $[S]$ values. K_m and V_{max} are then found from the median of all intersection points (orange stars). Use of the median rather than the mean minimizes the detrimental effect of outliers on parameter estimation (for further details see refs. 45 and 46). In practice, the intersection points are more easily found analytically from the equation of the lines with the help of a spreadsheet program. The direct linear plots depicted on the left and right panels were generated from the Michaelis-Menten plots shown in Fig. 8a at the concentrations of AuMBA indicated.